

Stability analysis of stratified rock slopes with spatially variable strength parameters: the case of Qianjiangping landslide

Huiming Tang¹ · Rui Yong² · M. A. M. Ez Eldin³

Received: 12 November 2015 / Accepted: 30 March 2016 / Published online: 11 April 2016
© Springer-Verlag Berlin Heidelberg 2016

Abstract Jurassic strata prone to slope failure are widely distributed in the Three Gorges Reservoir region. The limit equilibrium method is generally used to analyze the stability of rock slopes that have a single failure plane. However, the stability of a stratified rock mass cannot be accurately estimated by this method because different bedding planes have variable shear strength parameters. A modified limit equilibrium method is presented with variable water pressure and shear strength used to estimate the stability coefficient of a sloping mass of stratified rock and to identify the potential sliding surface. Furthermore, an S-curve model is used to define the spatial variations of the shear strength parameters c and ϕ of the bedding plane and the tensile strength of the rock mass. This model can also describe the variation of strength parameters with distance from the slope surface, which depends on the reservoir water level. Also, it is used to evaluate the stability of the Qianjiangping landslide, located at Shazhenxi Town, Zigui County, Three Gorges Reservoir area, China. The results show the most probable sliding surface is the interface between a slightly weathered layer and subjacent bedrock. When reservoir water rises above the elevation of the slide mass toe, the stability coefficient of the slope declines sharply. When the reservoir water level is static at 135 m,

the stability coefficient decreases gradually as the phreatic line changes as a result of heavy rainfall.

Keywords Stratified rock slope · Bedding plane · Slope stability · Plane failure · Limit equilibrium

Introduction

Rockslides are one of the most widespread and frequent hazards on Earth. Every year these disasters result in terrible loss of life and losses of billions of dollars, while also impacting socio-economic and cultural activities, communication and transport services, basic facilities and utilities, etc.

Stratified sedimentary rocks cover two thirds of Earth's land surface (77.3 % in China). Many stability problems of stratified rock result from human activities, and the frequency of related disasters is increasing. Planar failure is one of the most common causes of rockslides, and these generally occur in stratified rock masses (Gencer 1985; Dong et al. 2012; Ching et al. 2013). The stratified structure of a rock mass is typically acquired during sedimentary deposition, but planar structures such as foliation or schistosity can also be produced by metamorphism. This process can cause differences in material composition, particle size, fabric, or mineral orientation that results in rock stratification (Yang and Yin 2006). The dips and mechanical parameters of bedding planes thus formed in naturally stratified rocks have significant effects on rock mass strength and stability. Therefore, the appraisal of slope stability in stratified rock masses is complex because dominant discontinuities lead to a highly anisotropic behavior (Fortsakis et al. 2012).

The problem of rock slope stability is an active field of research in engineering, and much work involving many

✉ Rui Yong
yongrui_usx@hotmail.com; yongrui@usx.edu.cn

¹ Engineering Faculty, China University of Geosciences, Wuhan, Hubei 430074, People's Republic of China

² Civil Engineering Faculty, Shaoxing University, Shaoxing, Zhejiang 312000, People's Republic of China

³ College of Petroleum Geology and Minerals, University of Bahri, Khartoum 12327, Sudan

different methods has been devoted to this problem (Qin et al. 2001; Chen 2004; Eberhardt et al. 2005; Yang and Zou 2006; Li et al. 2008; Hammouri et al. 2008; Pantelidis 2009; Taghavi et al. 2010; Ghazvinian et al. 2013; Gong et al. 2013; Tiwari 2015). In general, the primary methods for rock slope stability analysis can be classified into the following categories: (1) conventional methods; (2) numerical simulation; and (3) in situ and model tests. Furthermore, the conventional methods are divided into kinematic analysis, limit equilibrium analysis, probability analysis, rock mass classification systems analysis, and physical modeling techniques. The numerical methods of rock slope analysis can be divided into continuum modeling (e.g., finite-element and finite-difference), discontinuum modeling (e.g., distinct-element and discrete-element), and hybrid modeling.

At present, the limit equilibrium method plays a major role in practical slope or landslide engineering because its simplicity endows it with advantages over more sophisticated analysis methods (Eberhardt et al. 2004; Li et al. 2008; Liu et al. 2008; Zhou and Cheng 2013; Xu and Wang 2015). Ching et al. (2013) proposed a model for the rock pressure induced by an excavation/cut in sedimentary rocks to account for sliding along parallel bedding planes. However, these methods are restricted by the requirement that single valued parameters describe the slope characteristics (Johari et al. 2013). In actuality, the shear strength of a rock mass is spatially variable due to differences in lithology, composition, weathering, discontinuities, climate, carbonation, relief, vegetation cover, and human activities. This inherent variability of shear strength affects the accuracy of slope stability calculations made by the limit equilibrium method. Furthermore, the limit equilibrium method is generally used to analyze the stability of rock slopes where a single failure plane is present. Many potential sliding surfaces exist in real stratified rock masses and these should be considered together to determine the stability coefficient.

This study develops a modified limit equilibrium method for determining the stability of stratified rock masses. Specifically, spatial variations of rock strength caused by discontinuities are introduced through this method. The change in rock strength along the bedding surface with reservoir water level is described by the S curve model. Meanwhile, this method introduces the idea of determining the spatial variations of rock strength and water pressure according to the phreatic line calculation in reservoir slope.

This method is used to study the stability of the Qianjiangping landslide, which is developed on Jurassic strata with weak interlayers. This landslide is located at Shazhenxi Town, Zigui County, Three Gorges Reservoir area, China (Fig. 1). It is situated about 5 km upstream of the confluence of the Qinggan River and the Yangtze River.

The landslide occurred only 43 days after the impoundment of the Three Gorges Reservoir. The calculations reveal the instability in the various processes and mechanisms of the landslide.

Spatial variation model of strength parameters of rock mass and rock discontinuities

Field investigations indicate that the cohesion c and friction angle ϕ of a bedding surface change at different slip surfaces. Moreover, as is common sense, the shear strength of rock discontinuities adjacent to a slope surface is usually lower than that at greater depth. This anisotropy of strength is also affected by spatial variations of the above-mentioned factors. Reservoir operations and engineering activities can cause significant variations in the moisture content and mechanical parameters of rock masses (Liu et al. 2004). Lu (2010) studied the variation rules of the rock discontinuity shear strength with different moisture contents. The strength of a rock mass can be affected by changing reservoir levels, but there is less influence deeper in the mass.

The shear strength of the potential failure plane determines the resistant force, thereby controlling the stability of the rock slope. However, the shear strength of rock discontinuities is treated as a constant in the original formula for planar failure analysis. Hence, the original method cannot be used to accurately analyze slope stability in dynamic situations.

The S-curve model, which describes the progressive transition from one value state to another, is often expressed in units of time or distance. This model has been widely used in statistical and empirical analysis in fields like sociology, biostatistics, clinical medicine, and marketing management. It has also been used to describe strength variations along landslide rupture surfaces (e.g., Tang et al. 2015). The variable of interest increases nonlinearly and continuously, such that the variation trend is shaped like the letter S. This characteristic is well suited for illustrating the variations of rock mass strength including shear strength parameters c and ϕ , as shown in Fig. 2.

According to the S-curve model, the strength can be defined as follows:

$$S(d) = \frac{A}{1 + e^{-r(d-b)}} + H, \quad (1)$$

where $S(d)$ denotes the strength of the rock mass or rock discontinuities, d is the distance to the slope surface along the bedding surface, and H is the lowest strength of the rock mass or rock discontinuities (saturation strength) usually occurring near the slope surface. The strength of the rock or discontinuities at greater depth or distance is little affected by the water, so it has a much higher value

Fig. 1 Location map of Qianjiangping landslide

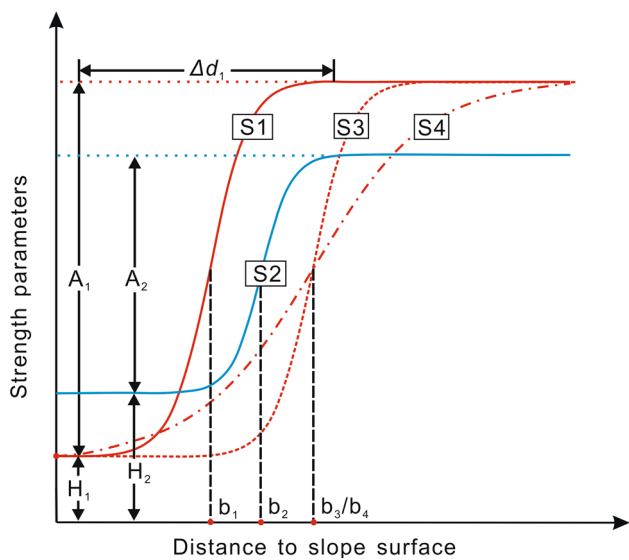


Fig. 2 Relationship between strength parameters and distance to slope surface

equal to $A + H$, where A is the difference between the lowest (saturation strength) and the highest (natural strength). The contrast between curves S1 and S2 in Fig. 2 illustrates the influence of coefficients A and H . Factors b and r are coefficients that control the position and shape of the S-curve. Factor b represents the distance to the slope surface when the strength is equal to the mean value of the lowest and the highest strength; this factor controls the position of the S curve, as illustrated by the contrast between S1 and S3 in Fig. 2. Factor r controls the rate of change between the lowest and highest values, and thus governs the shape of the S curve, as shown by the contrast between S3 and S4 in Fig. 2.

The shear strength parameters ϕ and c of a bedding plane are calculated in rectangular coordinate systems and the origin coordinate for each bedding plane is defined as its intersection with the slope face. On the basis of the S-curve model, the equations describing shear strength parameters ϕ , c along the bedding surface are:

$$\left. \begin{aligned} \phi(d) &= \frac{A_\phi}{1 + e^{-r_\phi(d-b_\phi)}} + H_\phi \\ c(d) &= \frac{A_c}{1 + e^{-r_c(d-b_c)}} + H_c \end{aligned} \right\} \quad (2)$$

where H_ϕ and H_c are the saturation shear strength of rock discontinuities. Also, A_ϕ and A_c are the differences between the saturation and nature shear strength parameters, and b_ϕ, b_c, r_ϕ , and r_c control the shape and midpoint position of the shear strength function. H_ϕ, H_c, A_ϕ , and A_c are obtained through sets of direct shear tests on specimens taken from the bedding surface.

The S curve reflects a gradual transition from one extreme value to another. The band width Δd is the interval where change occurs, starting from the lowest extreme value H and ending when the highest value $H + A$ is effectively attained. Zou et al. (2012) showed that Δd can be estimated if a limit of error δ is defined:

$$\delta = \frac{1}{e^{r\Delta d/2} + 1} \quad (3)$$

For example, assuming a limit of error $\delta = 0.1\%$, the value of $r\Delta d \approx 13.8$ can be obtained.

The shear strength parameters c and ϕ of the potential plane not only change with the distance to slope surface, but also change with time if the reservoir water level varies. Here, the parameter b of shear strength in S curve model is a function of time that can describe the stability evolution of rock slope as the reservoir level fluctuates. The shear strength parameters ϕ and c along the bedding surface can be illustrated by the following equations:

$$\left. \begin{aligned} \phi(d, t) &= \frac{A_\phi}{1 + e^{-r_\phi(d-b_\phi(t))}} + H_\phi \\ c(d, t) &= \frac{A_c}{1 + e^{-r_c(d-b_c(t))}} + H_c \end{aligned} \right\}, \quad (4)$$

where b_ϕ and b_c are calculated as follows:

$$b(t) = b_\phi(t) = b_c(t) = \frac{1}{2}(d_n(t) + d_s(t)) \quad (5)$$

In the above (see in Fig. 3), b is the distance from the slope surface to the intersection of the phreatic line and bedding surface. d_n is the distance from slope surface to the slope surface in natural state, and d_s is the distance from slope surface to the slope surface in the saturated state. Note that b is determined by calculating the phreatic line inside the reservoir slope.

Wu et al. (2009) derived an approximate analytical method to estimate the phreatic line position as a function of reservoir water level and rainfall. The initial value is a steady flow condition and the typical geological section is shown in Fig. 4.

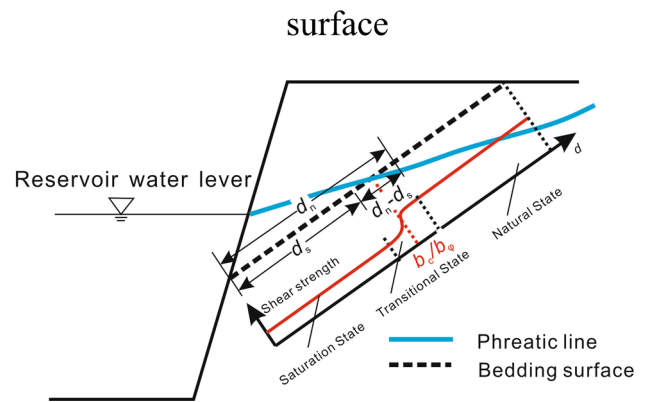


Fig. 3 Shear strength along the bedding surface

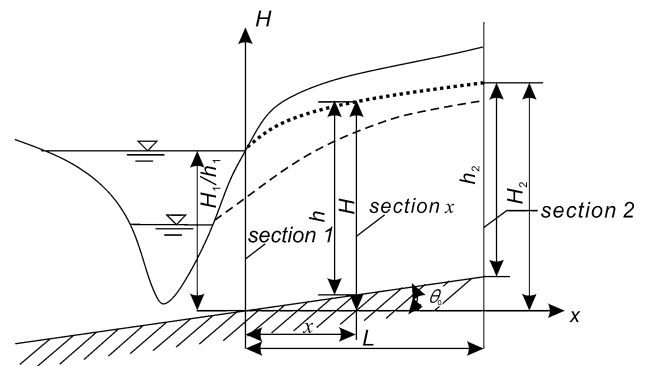


Fig. 4 Typical section of reservoir wall showing the variable position of the water table

The hydraulic head of the initial state is calculated as below, which is a modified Dupuit model, adjusted to accommodate a sloping impervious lower boundary:

$$H = x \tan \theta_0 + \sqrt{\frac{x}{L}(H_2^2 - H_1^2) + H_1^2 - xH_2 \tan \theta_0 + \frac{x^2}{4} \tan^2 \theta_0} \quad (6)$$

The parametric values for $H, h_1, h_2, H_1, H_2, L, x$, and θ_0 are shown in Fig. 4.

The hydraulic head of transient flow model is calculated as below:

$$H(x, t) = s(x, t) + H(x, 0) \quad (7)$$

in which

$$s(x, t) = vtR(\lambda) + \zeta t(1 - R(\lambda)) \quad (8)$$

Here $R(\lambda)$ is calculated as

$$\left. \begin{aligned} R(\lambda) &= (1 + 2\lambda^2) \operatorname{erfc}(\lambda) - \frac{2\lambda}{\sqrt{\pi}} e^{-\lambda^2} \\ \operatorname{erfc}(\lambda) &= \frac{2}{\sqrt{\pi}} \int_{\lambda}^{\infty} -e^{-t^2} dt; \lambda = \frac{x}{2\sqrt{at}} \\ a &= \frac{KH_m}{\mu} \end{aligned} \right\} \quad (9)$$

where K is average coefficient of permeability, H_m is the average height of aquifer, μ is the specific yield, v is the speed of water rise (+) or fall (-), and ζ is calculated from:

$$\zeta = \frac{w}{\mu}, \quad (10)$$

where w is the rainfall intensity.

Calculation method and model for stability analysis of bedding rock slope

Planar rock slope failure occurs when a mass of rock slides down and along a relatively planar, inclined failure surface. Such failure surfaces are usually structural discontinuities such as bedding planes, faults, joints, or the interface between bedrock and an overlying layer of weathered rock. Instability arises if the critical joint dip is less than the actual slope angle, which occurs when the shear strength of the joint is not sufficient to offset the driving forces.

The study of planar failure mechanisms provides insight into the behavior of rock slopes; the limit equilibrium approach is one of the most efficient ways to analyze the stability of a rock mass assuming incipient failure along a potential slip surface. In this method, the material above this surface is considered a “free body”. The disturbing and resisting forces are estimated, enabling the formulation of equations concerning force equilibrium or moment equilibrium (or both) of the potential slide mass. The stability coefficient is then defined as the ratio of resisting forces to driving forces.

Resisting forces include the shear strength of the failure plane and other stabilizing forces. The driving forces consist of the down-slope component of the weight of the slide block, forces generated by seismic acceleration or by water pressure acting on the block, and external forces on the lower slope surface.

Landslides in the reservoir area have gentle lower slopes and steep upper slopes. Many landslides, including Zhaoshuling Landslide, Hongshibao landslide, and the Huangtupo landslide, have the same topographic and geologic setting, and these masses have also been destabilized by human activities. The stability of such landslides can be analyzed by the typical double slip bedding surfaces based on their specific structure. The double planes below the sliding rock mass are analyzed by using the limit equilibrium method, as shown in the theoretical model (Fig. 5).

First, the reacting force R_1 acts on the bedrock under the sliding surface AB, and can be decomposed into the horizontal and vertical directions of the slope surface. The horizontal component force is R_{1h} and the vertical component force is R_{1v} .

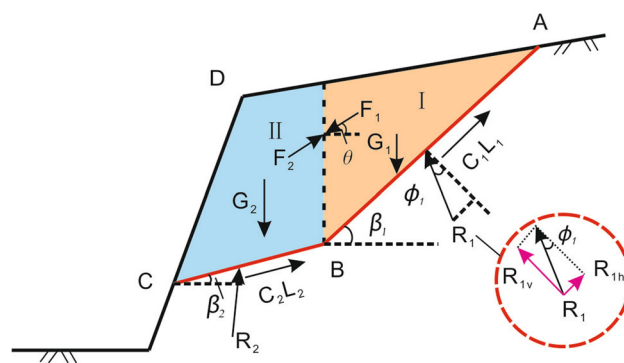


Fig. 5 Model of planar failure with double planes

$$\begin{cases} R_{1h} = G_1 \cos \beta_1 \tan \phi_1 \\ R_{1v} = G_1 \cos \beta_1 \end{cases} \quad (11)$$

Thus, R_1 can be estimated from:

$$R_1 = \sqrt{R_{1h}^2 + R_{1v}^2} = G_1 \cos \beta_1 \sqrt{\tan^2 \phi_1 + 1} \quad (12)$$

The stability coefficient η_2 of this kind of slope can be obtained from the following equation.

$$\eta_2 = \frac{G_2 \cos \beta_2 \tan \phi_2 + F_1 \sin(\theta - \beta_2) \tan \phi_2 + C_2 L_2}{G_2 \sin \beta_2 + F_1 \cos(\theta - \beta_2)}, \quad (13)$$

where ϕ_1 and ϕ_2 are the friction angle of the sliding surface AB and BC, G_1 and G_2 are the weight of the upper part (I) and the lower part (II), respectively, β_1 and β_2 are the dip angle of plane AB and BC, respectively, and F_1 is the reaction force applied by the upper part (I) with force direction angle θ ; $C_2 L_2$ is the resistant force caused by cohesion C_2 of slope surface with the length L_2 .

In this equation, the effect of water has not been taken into consideration. This is a limitation because in reservoir areas it is known that high water levels caused by impoundment can have an important, typically negative impact on slope stability, particularly if the level reaches the landslide toe. In particular, the lower part of the rupture surface is affected by variations of the reservoir water level, which can reduce its shear strength and increase the pore pressure.

Here, we attempt to develop a model that considers multiple layers, including the water effect; it also accounts for the spatial variability of strength parameters and the water pressure. The water level is assumed to have an effect on the lower plane. In order to give a brief derivation process, the weight of the upper part IG_{1i} and the lower part G_{2i} are given out directly.

In this model the bedding surface $A_i B_i C_i$ is assumed to be the failure surface (Fig. 6). The force of water U_{Si} , acting on the inundated part of the slope surface where area increases with the water level, is calculated as follows:

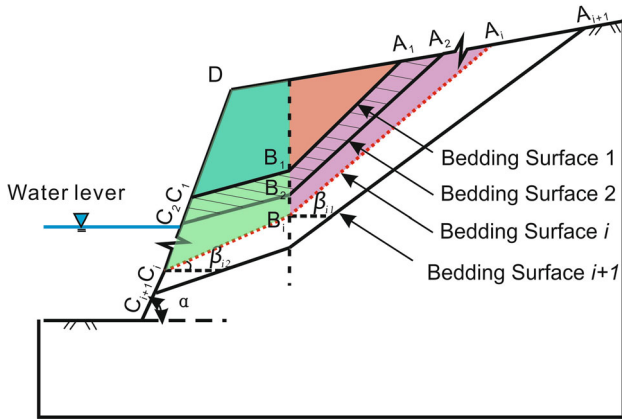


Fig. 6 Model of rock slope with bedding planes

$$U_{Si}(t) = \frac{1}{2} \gamma_w (h_w(t) - h_i)^2 / \sin \alpha \tag{14}$$

The U_S can be analyzed into two parts N_i , P_i perpendicular and parallel to the plane B_iC_i .

$$N_i(t) = U_{Si}(t) \cos(\alpha - \beta_{2i}) \tag{15}$$

$$P_i(t) = U_{Si}(t) \sin(\alpha - \beta_{2i}) \tag{16}$$

The water force acting on the plane B_iC_i , U_S , is calculated as follows:

$$U_{Bi}(t) = \frac{1}{2} \gamma_w (h_w(t) - h_i)(b(t) + \frac{1}{2} \Delta d) \tag{17}$$

The weakening effect on the shear strength of bedding surface caused by an increase in the reservoir level is considered as follows.

Firstly, the phreatic line inside the slope is calculated by Eq. (7). Comparing the result with the position of the bedding surface, the part remaining in the natural state can be determined. It is important to remember that the phreatic line calculations influence the sliding surface location and reveal how long it has been immersed in water.

Then Eq. (4) was used to calculate the distribution of the shear strength along the bedding surface. Then c_{1i} , c_{2i} , ϕ_{1i} , and ϕ_{2i} at different positions were obtained.

$$\left. \begin{aligned} c_{1i}(t)L_{1i} &= \int_0^{L_1} c_{i1}(x_1, t) dx_1 \\ \phi_{1i}(t) &= \frac{1}{L_1} \int_0^{L_1} \phi_{i1}(x_1, t) dx_1 \\ c_{2i}(t)L_{2i} &= \int_0^{L_2} c_{i2}(x_2, t) dx_2 \\ \phi_{2i}(t) &= \frac{1}{L_2} \int_0^{L_2} \phi_{i2}(x_2, t) dx_2 \end{aligned} \right\} \tag{18}$$

The F_{li} was analyzed into two components F_{ix} and F_{iy} : in horizontal and vertical directions, respectively.

$$F_{xi}(t) = G_{1i} \cos \beta_{1i} \sqrt{1 + \tan^2 \phi_{1i}} \sin(\beta_{1i} - \phi_{1i}) - C_{1i}(t)L_{1i} \cos \beta_{1i} \tag{19}$$

$$F_{yi}(t) = G_{1i} - G_{1i} \cos \beta_{1i} \sqrt{1 + \tan^2 \phi_{1i}} \cos(\beta_{1i} - \phi_{1i}) - C_{1i}(t)L_{1i} \sin \beta_{1i} \tag{20}$$

$$F_{li}(t) = \sqrt{F_{xi}(t)^2 + F_{yi}(t)^2} \tag{21}$$

$$\theta_i = \arctan \frac{F_{yi}(t)}{F_{xi}(t)} \tag{22}$$

The stability coefficient η_i of the slope was obtained by the following equation.

$$\left\{ \begin{aligned} \eta_i(t) &= \frac{W_{1i} + W_{2i} + W_{3i} + W_{6i} + W_{7i}}{W_{4i} + W_{5i}} \\ W_{1i} &= G_{2i} \cos \beta_{2i} \tan \phi_{2i}(t) \\ W_{2i} &= F_{li}(t) \sin(\theta_i - \beta_{2i}) \tan \phi_{2i}(t) \\ W_{3i} &= C_{2i}(t)L_{2i} \\ W_{4i} &= G_{2i} \sin \beta_{2i} \\ W_{5i} &= F_{li}(t) \cos(\theta_i - \beta_{2i}) \\ W_{6i} &= [-U_{Bi}(t) + N_i(t)] \tan \phi_{2i}(t) \\ W_{7i} &= P_i(t) \end{aligned} \right. \tag{23}$$

With these equations the most dangerous position for the potential slip surface was located by calculating the stability coefficient through a large number of trials. This is the surface that gives the minimum safety factor for the slope in conventional terms and is theoretically the critical slip surface. Moreover, the relationship between the stability of the rock slope and the reservoir level can be revealed by calculating the stability of the different layers.

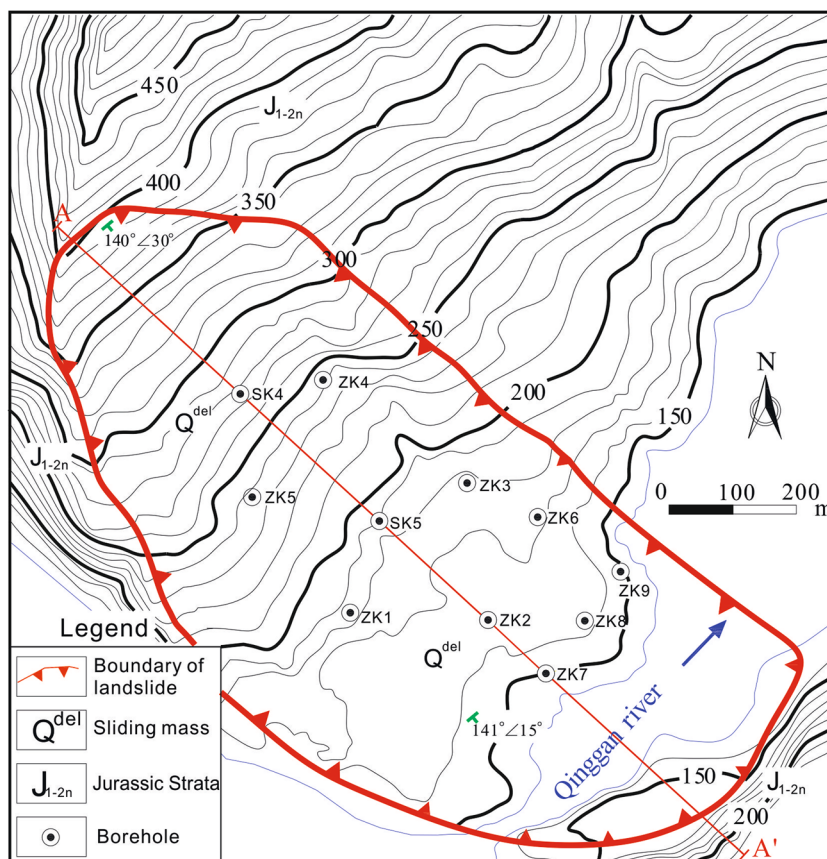
Case study of Qianjiangping landslide

Dimensions and features

The study area is a tectonically active region of middle and low mountains that is deeply incised by the Yangtze River and its tributaries. Steep slopes develop on soft, erodible, thin bedded sediments that are widespread in this area. Therefore, landslides are common, particularly near the major river channels.

Qianjiangping landslide developed along weak bedding planes in Jurassic strata that generally dip about 30° to the SE, down slope and toward the river. This tongue-shaped mass has a length of 1,150 m, a width of 600 m, and an average thickness of 30 m (in Fig. 7). The indicated total area is >0.69 km² and the volume is 21 × 10⁶m³. The main scarp has a maximum elevation of 450 m, but it

Fig. 7 Topography of the Qianjiangping landslide after 2003 (after Jian et al. 2014)



extends down to river level (Fig. 8, red dotted line). On July 14, 2003 the slide mass moved about 250 m toward S45° E, all within a period of 1–5 min. The slide mass is thinner in the main body and thicker at the foot. The dip angle of the lower rupture surface is mostly coincident with bedding in the upper part, but it becomes nearly horizontal at the toe of the landslide. Case histories show that slope failure in this region is common where the Jurassic strata have steep, downslope dips toward major rivers.

The landslide is bounded to the east, south, and west by a pronounced incised meander in the Qinggan River, a tributary of Yangtze River (Fig. 8). The water level of the Qinggan River rose from 95 m to 135 m in June 2003, immediately after impoundment of the Three Gorges reservoir and only a few weeks before the landslide event.

Geology and structure

The Qianjiangping landslide is a bedding controlled landslide. The local stratigraphic section is, from top to bottom, alluvium, clay, and gravel of Quaternary age, feldspathic quartz sandstone of Upper Jurassic–Cretaceous age, and fine sandstone with carbonaceous shale, siltstone with mudstone, and silty mudstone of the Middle to Lower Jurassic Niejiashan formation (J_{1-2n}). The sandstone is interbedded with

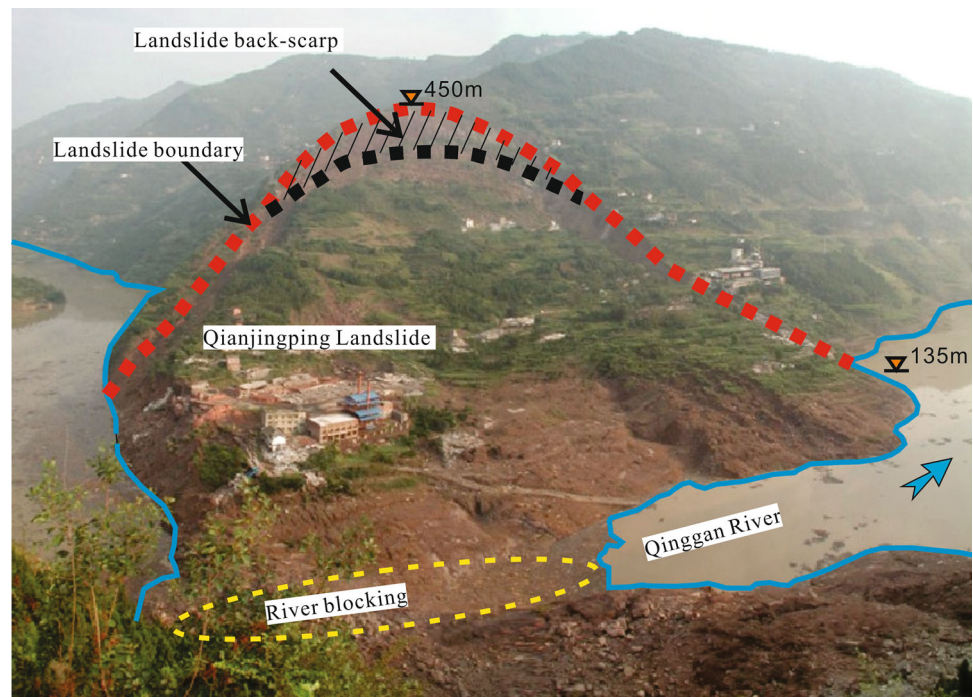
weak silty mudstone and shale layers. The greater region is structurally complex and tectonically active. The rapid incision of the Yangtze River, thought to have occurred in response to Quaternary tectonic uplift (Li et al. 2001; Fouriadis and Liu 2007; Li et al. 2012), has produced unstable slopes along its banks in numerous places. Field investigations show that fractures and discontinuities are abundant in the slightly weathered bedrock. The dip direction of the strata is reversed near the Qinggan River.

Hydrology and Hydrogeology

The Qinggan River has several tributaries and gullies. The gullies usually are dry but carry significant intermittent flows during the rainy season. The north bank of the Qinggan River, proximal to the landslide is a consequent slope with dip angle between 20° and 30°, while the south bank slope is an obsequent topographic surface.

Groundwater data in the vicinity of the landslide are limited. Data obtained from the bore holes on the landslide show that the phreatic zone within the slope material is very deep below the surface. Artesian contact springs were observed along planes of discontinuities and contacts between the dipping sandstone and mudstone units. Groundwater recharge and levels are mainly controlled by

Fig. 8 Front view of the landslide, looking NW (after Jiang et al. 2012)



the amount of rainfall, the infiltration rate and the level of reservoir water. Additionally, boring revealed that a highly fractured, 1–2 m-thick zone of bedrock immediately underlies the main slip zone, while the deeper bedrock was only slightly fractured; this indicates that the bedrock immediately below the slip zone is much more permeable.

Possible factors of promoting sliding

Qianjiangping landslide was a result of both internal and external factors. Internal factors include the loose accumulation of the slide mass, significant geomorphic features, and weak bedding surfaces. External factors include the sharp rise of the reservoir water level in June 2003, coincident with the heavy rainfall season.

Qianjiangping landslide occurred immediately after a period of nearly continuous rainfall from June 21 to July 11 in 2003. Also, the water level of the Qinggan River rose rapidly from 95 m to 135 m above sea level (asl) shortly after impoundment of the Three Gorges reservoir, which was initiated on June 1, 2003 (see below; Jian et al. 2014).

Many studies show that this landslide was triggered by the combined effect of this reservoir water rise and heavy rainfall. Groundwater data around the Qianjiangping landslide area and its environs are limited, but it is clear that the groundwater level near the toe of the landslide was influenced by the rapid increase in the reservoir level. This effect further triggered the destabilization of the mass.

The erosion by the river at the toe of the slope also decreased the stability of the slope. Based on these reasons,

the following failure analysis process primarily focuses on the rainfall effect and water effect caused by reservoir impoundment at the foot of the sliding zone.

Basic mechanism analysis

With the rising of the reservoir water level and the rainfall effect, the water gradually seeped from the slope surface into the interior of landslide body and the water capacity inside the slope changed in different reservoir filling stages. According to the laboratory investigations by Cao et al. (2007) and Li et al. (2013), the shear strength and deformation properties of slip zone soils of Qianjiangping landslide were highly influenced by the variations in soil moisture. The reservoir impoundment mainly affected the foot of Qianjiangping landslide, the effect of shear strength reduction at the foot of the slide mass was the most crucial factor in the landslide's initiation. The shear strength weakening of the slip zone in the lower layers of this landslide was demonstrated to have the strongest influence on the landslide's stability (Wen et al. 2008). More specifically, the lower layers were gradually soaked in water during the reservoir filling process. Affected by saturation and softening effects by water, the strength of slide mass and sliding zone would decrease correspondingly, reducing the stability of the slope. Also, with the water level increasing, the buoyant force at the lower layers also decreased the resistance force at the slope-toe. (Wang et al. 2008). The variations of resistance force changed the mechanical balance of slide mass and resulted in the slope

failure which developed along bedding planes of weak rocks. Thus, the Qianjiangping landslide occurred due to the combined influence of impoundment of Three Gorges reservoir and durative rainfall.

Failure process analysis of the landslide

Site investigations immediately following the landslide event report that the factory buildings on the slide mass and trees in the middle of the landslide remained standing. This observation indicates that the angle of the sliding surface remained constant, and no rotation occurred. The stabilities of sedimentary rock masses are typically controlled by the topographic slope and dipping bedding planes. The stability of this type of slope can be analyzed by the limit equilibrium method.

Furthermore, with reference to the degree of borehole data and weathering of the strata, the slide mass can be divided into two layers from top to bottom.

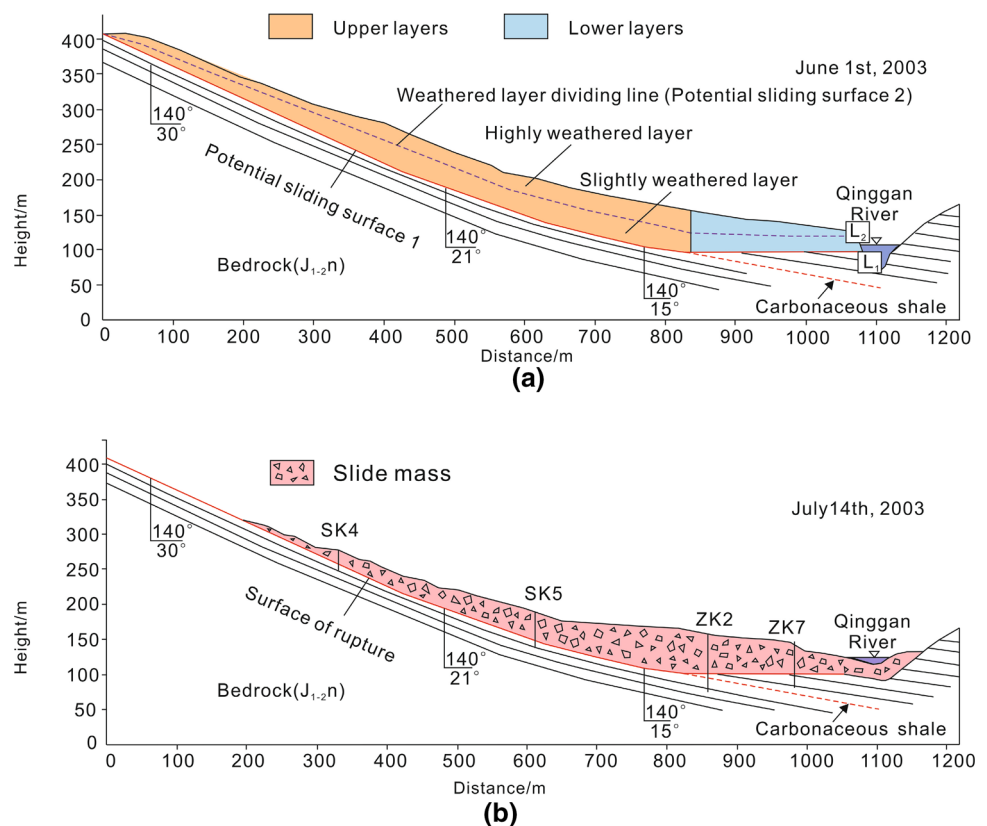
(1) The highly weathered layer is a loose, 5–15 m thick aggregate that includes fragments of Middle Jurassic mudstone and argillaceous siltstone enclosed in a matrix of clay and alluvial material. (2) Beneath this is a 20.0–40.0 m thick zone of slightly weathered, Middle Jurassic muddy siltstone and fine sandstone. Fractures are well developed, but the rocks and bedding remain intact.

The geological parameters of the slide mass are different in highly the weathered layer and slightly weathered layer. In the highly weathered layer, the saturated unit weight is 23.5 kN/m^3 ; the bulk modulus is $6.94 \times 10^8 \text{ Pa}$; the shear modulus is $1.81 \times 10^8 \text{ Pa}$; the cohesion is 100 kPa ; the friction angle of 30° ; the tension strength is $2 \times 10^6 \text{ Pa}$. Moreover, in the highly weathered layer, the saturated unit weight is 25.5 kN/m^3 ; the bulk modulus is $1.11 \times 10^{10} \text{ Pa}$; the shear modulus is $4.55 \times 10^9 \text{ Pa}$; the cohesion is 150 kPa ; the friction angle of 40° ; the tension strength is $4 \times 10^6 \text{ Pa}$ (Luo et al. 2007). According to grain size distribution of the slip zone soils by Cao et al. (2007), the grain size over 2 mm is 49–53 %. The natural density and dry density of the slip zone soil are 2.03 and 1.79 g/cm^3 , respectively; water content is 13.5 %; void ratio is 0.52; the degree of saturation is 70.2 %; the liquid limit is 34.7 %; and plastic limit is 18.3 %.

Based on the geological data and characteristic features on the landslide, a general pre-failure topographic and geological profile of the Qianjiangping slope can be inferred (Fig. 9). Before calculation, it is assumed that both the weathered layer dividing surface and the top surface of the bedrock are potential sliding surfaces.

Wen et al. (2008) performed a sensitivity analysis to evaluate the contribution of various sliding factors. The study reveals that the stability of Qianjiangping landslide is

Fig. 9 Reconstructed geological cross-section of the Qianjiangping landslide, **a** reconstructed before failure, and **b** after failure



most sensitive to cohesion at the foot of the landslide’s slip zone, followed by uplift pressure, internal friction angles of the zone, and the unit weight of the slide mass material. Reservoir impoundment mainly influenced the foot of the Qianjiangping landslide. The study also found that the effect of shear strength reduction at the foot of the slide mass was the most crucial factor in the landslide’s initiation.

Water is the most sensitive factor affecting the shear strength. The spatial variability of strength parameters has been introduced in the force equilibrium and failure plane strength principles. Water level data obtained from the Three Gorges Reservoir (Fig. 10) shows that the history of reservoir filling can be divided into three stages. In our calculations, we chose the Carbonaceous shale as the water resisting layer with the dip of 11.18°; average coefficient of permeability $K = 0.58$ m/d, average height of aquifer $H_m = 64.48$ m and specific yield $\mu = 0.032$; the speed of water rise $v_1 = 0.247$ m/d (Stage 1), $v_2 = 3.152$ m/d (Stage 2), and $v_3 = 0$ m/d (Stage 3); the rainfall intensity $w_1 = 0$ mm/d (Stage 1), $w_2 = 0$ mm/d (Stage 2), and $w_3 = 5.667$ mm/d (Stage 3).

Phreatic lines inside the reservoir slope were calculated by Eq. (7). The results (Fig. 11) show the relationship between the phreatic line and two potential failure surfaces from May 1 to July 13 before the Qianjingping landslide occurred.

In Fig. 11, 1074 m at the slope surface represents the river shore, a position corresponding to Fig. 4 the distance (0). Also, b is the parameter of the S curve model mentioned in Eq. (5).

The intersections of the phreatic line and the potential sliding surfaces were calculated, including the position of

the highly weathered and slightly weathered layers (Figs. 12, 13, 14).

$$b'_1 = 8.14t + 0.48 \tag{24}$$

$$b'_2 = 12.85t + 2.12 \tag{25}$$

$$b''_1 = 44 \tag{26}$$

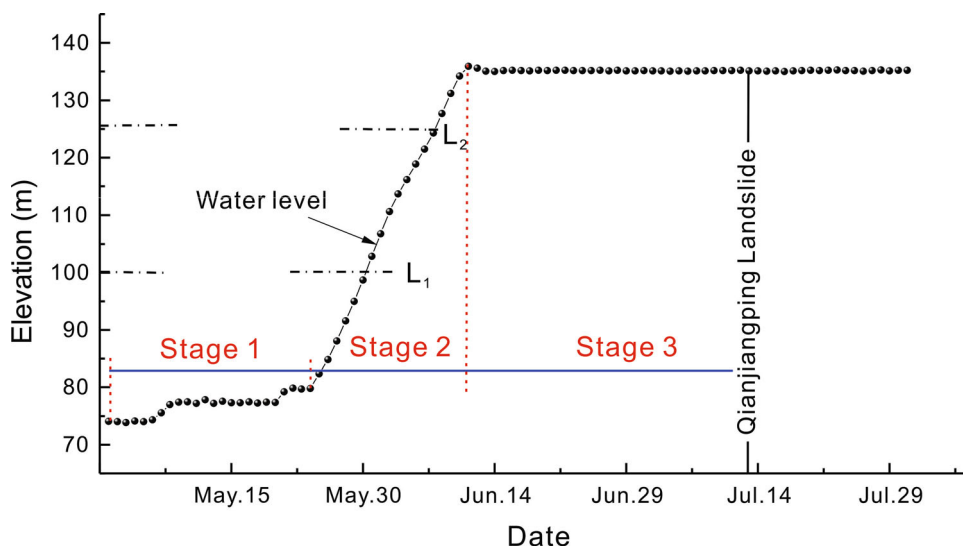
$$b''_2 = 2.52t + 150.17 \tag{27}$$

The bandwidth Δd in the S curve model, representing the distance from the natural state to the saturation state, is 22 meters.

According to the limit of error δ disused before, the value of $r\Delta d \approx 13.8$. So the parameter $r = 0.627$ can be obtained.

As can be observed (Figs. 15, 16), the friction angle and cohesion of both potential sliding surfaces of the lower layer were unchanged in Stage 1 (May 1–24, 2003). In Stage 2 (May 25–June 11, 2003), the friction angle and cohesion remained constant along the potential sliding surface 1 from May 25 to June 30, and then a gradual transition on the strength distribution along the sliding surface appeared. From May 31 to June 11, the shear strength declined to the saturation value in the areas immersed in water and the shear strength kept the natural value in other part of the potential sliding surface at the lower part of Qianjiangping landslide. By contrast, as the potential sliding surface 2 is higher than surface 1, the shear strength distribution was not affected by the water until June 5. Thus, the distribution changed during the period from June 6 to June 11. In Stage 3 (June 12–July 13, 2003), with growing areas of the potential sliding surface 1 submerging in water, the saturation shear strength spread along most part of the sliding surface. In Fig. 11c, the

Fig. 10 The conditions of water level rise from May 24 to July 14, 2003. Water levels from Three Gorges Co. (2014). Lines L1 and L2 refer to the levels on the landslide toe as shown in Fig. 9



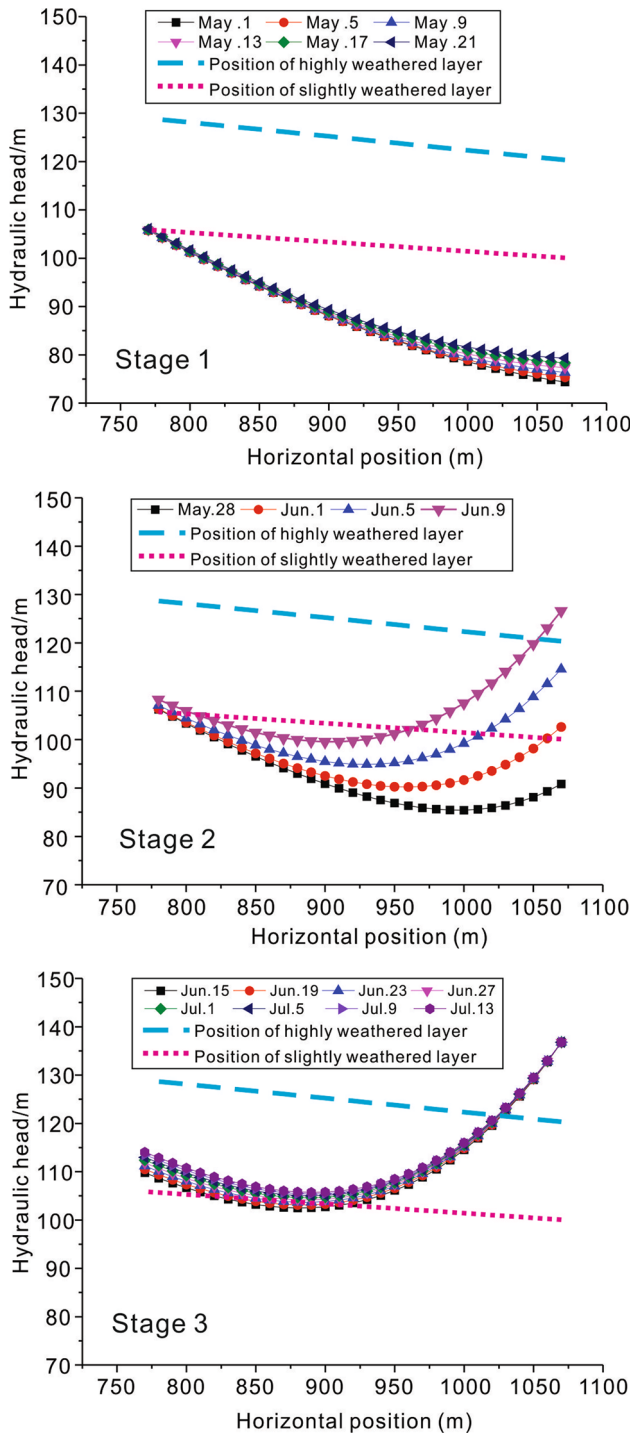


Fig. 11 Phreatic lines inside the slope calculated by Eqs. 6–10 before the Qianjingping landslide event. **a** Stage 1 (May 1–24, 2003); **b** Stage 2 (May 25–June 11, 2003); **c** Stage 3 (June 12–July 13, 2003). The horizontal axis represent horizontal locations inside of the landslide to the north shore of the river at 1074 m

intersection of the phreatic line and bedding surface showed little change in Stage 3, and therefore, the friction angle and cohesion distributions along the potential sliding

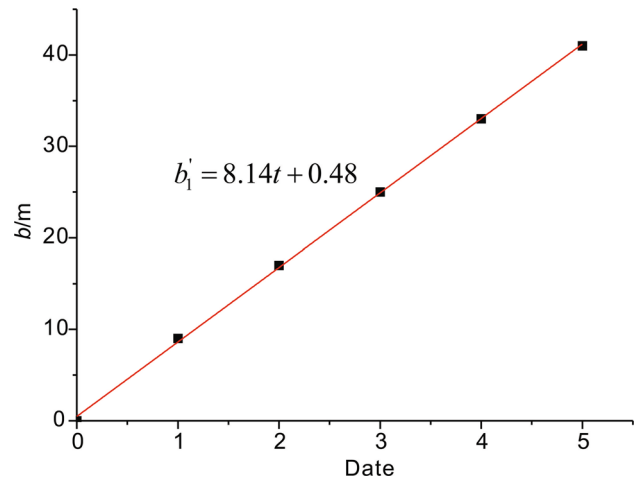


Fig. 12 Parameter b'_1 in S curve model fitting from June 6 to June 11

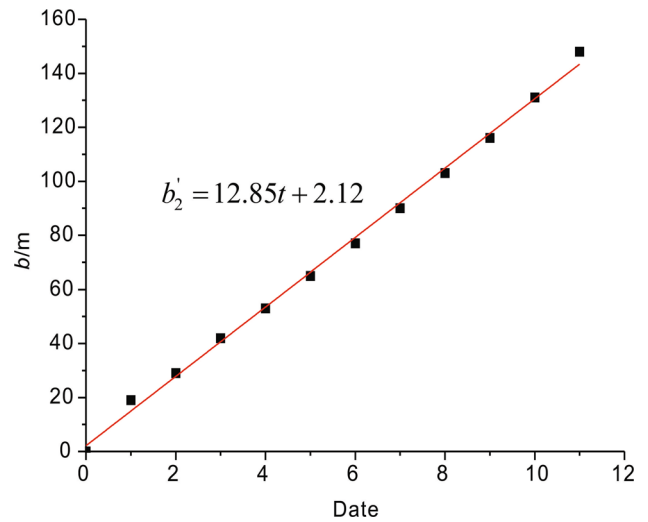


Fig. 13 Parameter b'_2 in S curve model fitting from May 31 to June 11

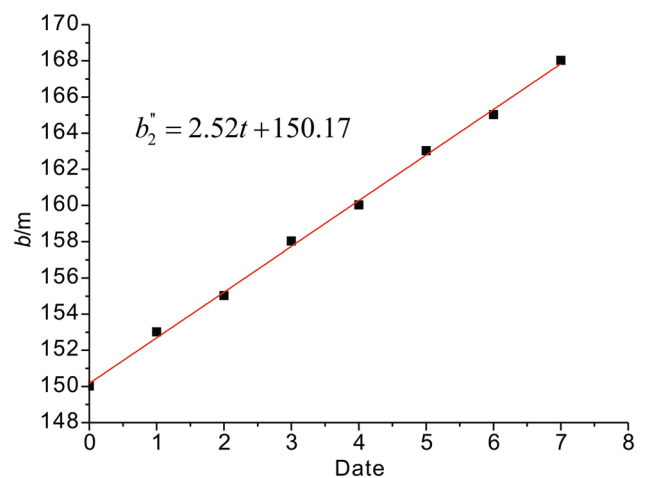


Fig. 14 Parameter b'' in S curve model fitting from June 11 to July 13

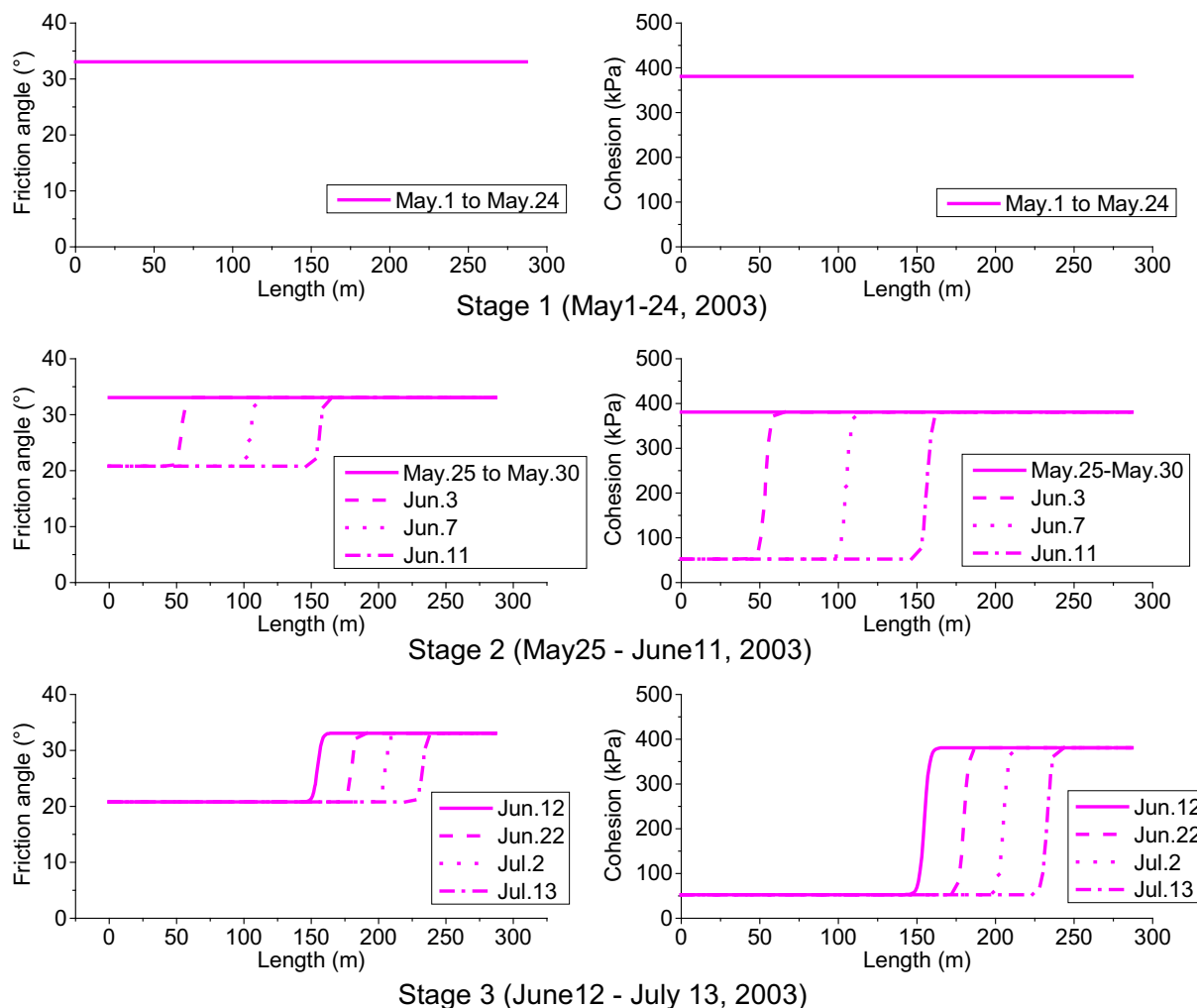


Fig. 15 The friction angle and cohesion distributions along the potential slide surface 1 of the lower layer before the Qianjiangping landslide event

surface 2 of the lower layer maintained the same as the situation at the end of Stage 2.

The unit volume of the upper highly weathered layer V_1 is 19,500 m³, the unit volume of the upper slightly weathered layer V_2 is 23,100 m³, the unit volume of the lower highly weathered layer V_3 is 3433 m³, and the unit volume of the lower slightly weathered layer V_4 is 6467 m³. The unit weight of the highly weathered layer and the slightly weathered layer are 22.5 kN/m³ and 24.5 kN/m³, respectively. The shear strength components of upper and lower layers of Qianjiangping landslide are tabulated in Tables 1, 2.

Detailed stability analysis is performed to quantify the degree of stability of the Qianjiangping slope using the modified limit equilibrium method for the case of double slip bedding surfaces. The result of the stability coefficient is presented in Fig. 17.

The impoundment of Three Gorges Reservoir began on June 1, 2003. The water level of the Qinggan River rose

rapidly to almost 135 m by June 16, 2003 (Fig. 10). During this period, the stability coefficient of the lower bedding surface declined sharply from 1.77 to 1.28. The stability coefficient of the upper bedding surface declined slowly until the water level reached the front part of these beds on June 6, 2003. Before that time, the stability coefficient was nearly static and the water effect was not obvious. After June 16, the reservoir water level was maintained at 135 m. Subsequently the stability coefficient of the lower bedding surfaces declined slowly, being affected only by the retrogression of bedding surface shear strength caused by the rainfall effect.

The curve for stability coefficient variations shows that the stability of the upper bedding surface was smaller than the lower surface before June 18. However, the stability of the upper bedding surface was higher than the lower surface during the rest of the time. Overall, the stability coefficient decline rate of the upper bedding surface is smaller than that of lower one.

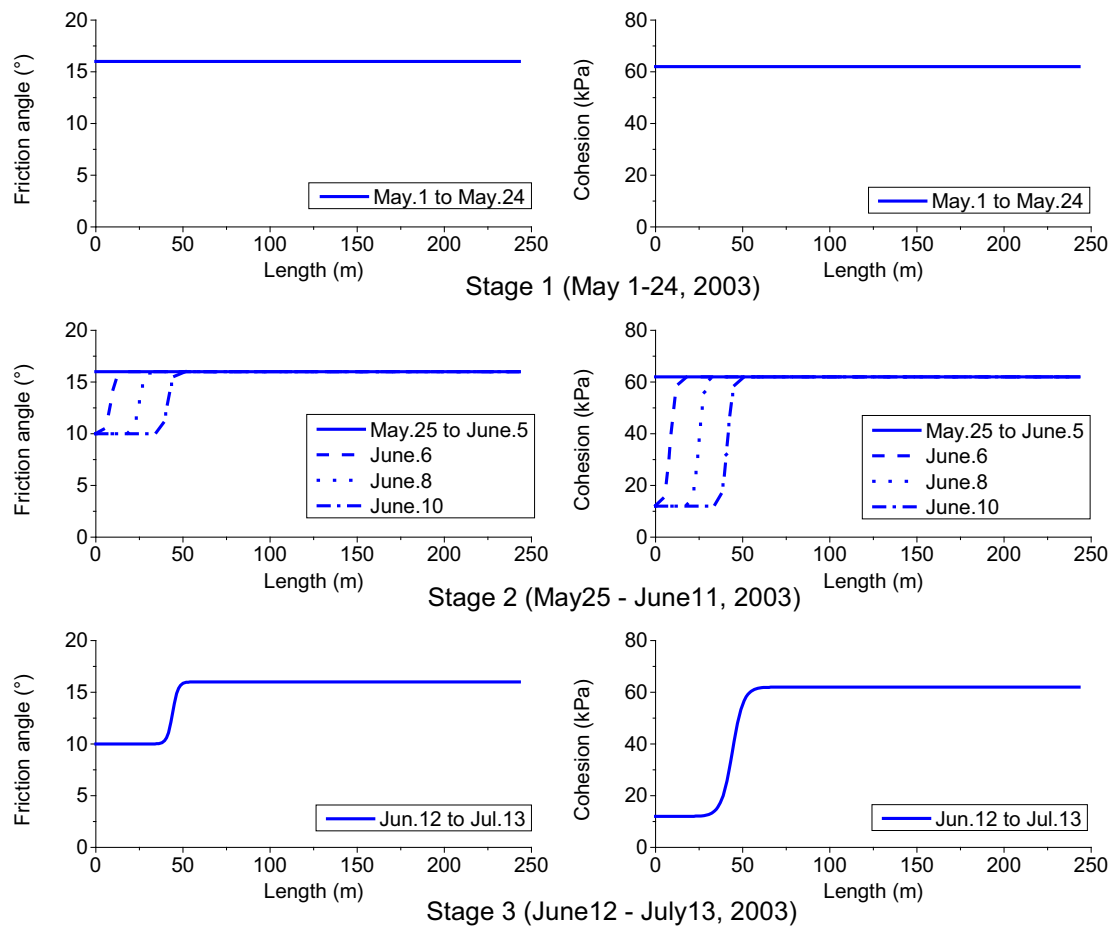


Fig. 16 The friction angle and cohesion distributions along the potential slide surface 2 of the lower layer before the Qianjiangping landslide event

Table 1 Shear strength components of upper layers of Qianjiangping landslide

Slip zone	length (m)	Dip angle (°)	Cohesion (kPa)	Internal friction angle (°)
Potential sliding surface 1	864.88	18.55	65.00	16.00
Potential sliding surface 2	830.09	22.87	15.00	11.00

Table 2 Shear strength components of lower layers of Qianjiangping landslide

Slip zone	length (m)	Dip angle (°)	H_c (kPa)	A_c (kPa)	H_f (kPa)	A_f (kPa)
Potential sliding surface 1	242.67	1.65	12	50	10	6
Potential sliding surface 2	286.68	1.12	52.80	328.2	20.8	12.3

Therefore, our model shows that the lower bedding surface is the most probable sliding surface, in accord with observation.

On July 12, the stability coefficient of the lower bedding surface declined to 0.998 which means the slope became critical. Field investigations indicate that the slope underwent large deformation. On July 13, the stability coefficient of the lower bedding surface declined to 0.989, and the landslide occurred along this surface in the early morning, nearly at 00:20 on July 14, 2003.

Discussion

The Three Gorges Project (TGP) in Hubei Province, China, is the one of the largest hydro-development projects in the world. Slope instability is a recurring problem in this area due to the presence of thin layers of mud and carbonaceous shale intercalated with siltstone and sandstone beds. These lenses are considered very weak zones, especially in the presence of water, and function as sliding surfaces when a considerable amount of water is absorbed.

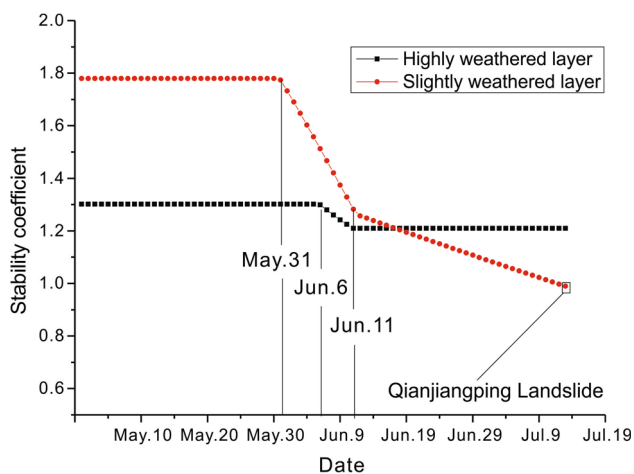


Fig. 17 A representation of stability coefficients for sliding mass under different layers with changing water levels

Landslides in the reservoir area always have steep upper slopes and gentle lower slopes. Therefore, it is important to evaluate reservoir landslides and the effect of reservoir level variations and rainfall. Stability analysis can be made for the case of double slip bedding surfaces in a stratified setting.

The spatial variation of strength parameters of rock mass and rock discontinuities discussed in this paper is based on the S-curve model. This model is a straightforward way to estimate the spatial variability of shear strength parameters c and ϕ . Furthermore, in this modified limit equilibrium model for stratified rock masses, the strength spatial variations of rock discontinuities, and rock mass are introduced. Note here that this strength parameter model of rock mass and rock discontinuities sometimes cannot exactly describe the spatial variability of strength parameters. Nevertheless, the main idea of stability coefficient calculation for a stratified rock slope is still valid and variable strength parameters are required inputs.

The sliding surface of an unstable rock mass may consist of a single plane that underlies the entire landslide or a complex surface that includes both discontinuities and fractures through intact rock (Duncan and Christopher 2005). Here, the sliding surface is determined by the bedding surface, which is different from the failure mode, in which the propagating cracks could extend and coalesce with neighboring joints resulting in the development of a continuous failure plane. The method developed in this paper is appropriate for analyzing the stability of stratified rock slope with an undeveloped main joint crack.

Conclusion

A modified limit equilibrium method for predicting the stability of a sedimentary rock slope with flat bedding planes is proposed with double slip bedding surfaces. This method

provides a more realistic way to calculate the stability factor of bedding rock slopes than the conventional limit equilibrium method because: (1) the phreatic line inside the reservoir wall is considered; (2) the spatial variability of strength parameters of bedding plane discontinuities is also considered; (3) variations of the strength functions are accounted by the S curve model; (4) the effect of water pressure acting on the slope surface and different bedding layers is included; and (5) the effect of shear strength reduction of the bedding surface is reflected by the variability of strength parameters in time and space by S curve model.

The impoundment of the Three Gorges reservoir clearly destabilized many landslide masses including the Qianjiangping landslide. The stability coefficients of slide mass with different layers and water level fluctuations reveal that the weakening of the bedding surface caused by rising reservoir water and heavy rainfall played an important role in the landslide occurrence. The bedding surface of carbonaceous shale between the unweathered layer and slightly weathered one turned out to be the most probable sliding surface.

The modified limit equilibrium method can inform reservoir managers and can help to evaluate the stability of stratified rock slope masses in reservoir areas.

Acknowledgments This study is financially supported by the National Basic Research Program 973 Project of the Ministry of Science and Technology of the People's Republic of China (2011CB710604), National Natural Science Foundation of China (No. 41272305), National Natural Science Foundation of China (No. 41502300), Zhejiang Provincial Natural Science Foundation (No. Q16D020005). The authors appreciate the help provided by Harkiran Kaur, who made the careful English language editing on this manuscript before submitting.

References

- Cao L, Luo XQ (2007) Experimental study of dry-wet circulation of Qianjiangping Landslide's unsaturated soil. *Rock Soil Mech* 28:93–97 (in Chinese)
- Chen Z (2004) A generalized solution for tetrahedral rock wedge stability analysis. *Int J Rock Mech Min Sci* 41:613–628
- China Three Gorges Corporation. (2014) Title: Hydrologic situation, <http://www.ctg.com.cn/inc/sqsk.php>
- Ching J, Yang ZY, Shiau JQ, Chen CJ (2013) Estimation of rock pressure during an excavation/cut in sedimentary rocks with inclined bedding planes. *Struct Saf* 41:11–19
- Dong JJ, Tu CH, Lee WR, Jheng YJ (2012) Effects of hydraulic conductivity/strength anisotropy on the stability of stratified, poorly cemented rock slopes. *Comput Geotech* 40:147–159
- Duncan CW, Christopher WM (2005) *Rock slope engineering—civil and mining*, 4th edn. Taylor & Francis e-Library, New York, pp 22–55
- Eberhardt E, Stead D, Coggan JS (2004) Numerical analysis of initiation and progressive failure in natural rock slopes—the 1991 Randa rock slide. *Int J Rock Mech Min Sci* 41:69–87
- Eberhardt E, Thuro K, Luginbuehl M (2005) Slope instability mechanisms in dipping interbedded conglomerates and

- weathered marls—the 1999 Rufi landslide, Switzerland. *Eng Geol* 77:35–56
- Fortsakis P, Nikas K, Marinos V, Marinos P (2012) Anisotropic behavior of stratified rock masses in tunnelling. *Eng Geol* 141–142:74–83
- Fourniadis IG, Liu JG (2007) Landslides in the Wushan–Zigui region of the Three Gorges, China. *Q J Eng Geol Hydroge* 40:115–122
- Gencer M (1985) Progressive failure in stratified and jointed rock mass. *Rock Mech Rock Eng* 18:267–292
- Ghazvinian A, Vaneghi RG, Hadei MR, Azinfar MJ (2013) Shear behavior of inherently anisotropic rocks. *Int J Rock Mech Min Sci* 61:96–110
- Gong WL, Wang J, Gong YX, Guo PY (2013) Thermography analysis of a roadway excavation experiment in 60° inclined stratified rocks. *Int J Rock Mech Min Sci* 60:134–147
- Hammouri NA, Malkawi AIH, Yamin MM (2008) Stability analysis of slopes using the finite element method and limiting equilibrium approach. *Bull Eng Geol Environ* 67:471–478
- Jian WX, Xu Q, Yang HF, Wang FW (2014) Mechanism and failure process of Qianjiangping landslide in the Three Gorges Reservoir, China. *Environ Earth Sci* 72(8):2999–3013
- Jiang QH, Zhang ZH, Wei W, Xie N, Zhou CB (2012) Research on triggering mechanism and kinematic process of Qianjiangping landslide. *Dis Adv* 5(4):631–636
- Johari A, Fazeli A, Javadi AA (2013) An investigation into application of jointly distributed random variables method in reliability assessment of rock slope stability. *Comput Geotech* 47:42–47
- Li JJ, Xie SY, Kuang MS (2001) Geomorphic evolution of the Yangtze Gorges and the time of their formation. *Geomorphology* 41:125–135
- Li AJ, Merified RS, Lvamin AV (2008) Stability charts for rock slopes based on the Hoek-Brown failure criterion. *Int J Rock Mech Min Sci* 45:689–700
- Li CD, Hu XL, Tang HM, Fan FS, Wang LQ (2012) Evaluation and control study on reservoir bank landslide in the Three Gorges reservoir region, China. *Disa Adv* 5(4):8–135
- Li YR, Wen BP, Aydin A, Ju NP (2013) Ring shear tests on slip zone soil zone soils of the three giant landslides in the Three Gorges Project area. *Eng Geol* 154:106–115
- Liu JG, Mason PJ, Clerici N, Chen S, Davis A, Miao F, Deng H, Liang L (2004) Landslide hazard assessment in the Three Gorges area of the Yangtze river using ASTER imagery: Zigui-Badong. *Geomorphology* 61:171–187
- Liu CH, Jaksa MB, Meyers AG (2008) Improved analytical solution for toppling stability analysis of rock slopes. *Int J Rock Mech Min Sci* 45:1361–1372
- Lu ZD (2010) Experimental and theoretical analysis on mechanical properties of fractured rock under water-rock interaction. Ph.D. Thesis, Wuhan China
- Luo XQ, Xu KX, Xiao SR, Wang ZJ, Zhang ZH (2007) The formation mechanism of Qianjiangping landslide in the Three Gorges Reservoir, China. Research report, pp 13–69 (in Chinese)
- Pantelidis L (2009) Rock slope stability assessment through rock mass classification systems. *Int J Rock Mech Min Sci* 46:315–325
- Qin S, Jiao JJ, Wang S, Long H (2001) A nonlinear catastrophe model of instability of planar-slip slope and chaotic dynamical mechanisms of its evolutionary process. *Int J Solids Str* 38:8093–8109
- Taghavi M, Dovoudi MH, Amiri-Tokaldany E, Darby SE (2010) An analytical method to estimate failure plane angle and tension crack depth for use in riverbank stability analyses. *Geomorphology* 123:74–83
- Tang HM, Zou ZX, Xiong CR, Wu YP, Hu XL, Wang LQ, Lu S, Criss RE, Li CD (2015) An evolution model of large consequent bedding rockslides, with particular reference to the Jiweishan rockslide in Southwest China. *Eng Geol* 186(24):17–27
- Tiwari R (2015) Simplified numerical implementation in slope stability modeling. *Int J Geomech* 15(3):1–19
- Wang FW, Zhang YM, Huo ZT, Peng XM, Wang SM, Yamasaki S (2008) Mechanism for the rapid motion of the Qianjiangping landslide during reactivation by the first impoundment of the Three Gorges Dam reservoir, China. *Landslides* 5:379–396
- Wen B, Shen J, Tan J (2008) The influence of water on the occurrence of Qianjiangping landslide. *Hydrogeol Eng Geol* 3:3–18
- Wu Q, Tang HM, Wang LQ, Lin ZH (2009) Analytic solutions for phreatic line in reservoir slope with inclined impervious bed under rainfall and reservoir water level fluctuation. *Rock Soil Mech* 30(10):3025–3031
- Xu B, Wang Y (2015) Stability analysis of the Lingshan gold mine tailings dam under conditions of a raised dam height. *Bull Eng Geol Environ* 74:151–161
- Yang XL, Yin JH (2006) Linear Mohr-Coulomb strength parameters from the non-linear Hoek-Brown rock masses. *Int J Nonlin Mech* 41:1000–1005
- Yang XL, Zou J (2006) Stability factors for rock slopes subjected to pore water pressure based on Hoek-Brown failure criterion. *Int J Rock Mech Min Sci* 43:1146–1152
- Zhou XP, Cheng H (2013) Analysis of stability of three-dimensional slopes using the rigorous limit equilibrium method. *Eng Geol* 160:21–33
- Zou ZX, Tang HM, Xiong CR, Wu YP, Liu X, Liao SB (2012) Geomechanical Model of progressive failure for large consequent bedding rockslide and its stability analysis. *Chin J Rock Mech Eng* 31(11):2222–2230 (in Chinese)